Inorg. Chem. **2006**, *45*, 2979–2988

Inorganic Chemistry Article

Analogue Reaction Systems of Selenate Reductase

Jun-Jieh Wang, Christian Tessier, and R. H. Holm*

Department of Chemistry and Chemical Biology, Harvard University, Cambridge, Massachusetts 02138

Received December 20, 2005

Analogue reaction systems of selenate reductase, which reduces substrate in the overall enzymatic reaction $SeO_4^{2-} + 2H^+ + 2e^- \rightarrow SeO_3^{2-} + H_2O$, have been developed using bis(dithiolene) complexes of Mo^{IV} and W^{IV}. On the basis of the results of EXAFS analysis of the oxidized and reduced enzyme, the minimal reaction $Mo^{IV}OH + SeO_4^{2-} \rightarrow Mo^{VI}O(OH) + SeO_3^{2-}$ is probable. The square pyramidal complexes $[M(OMe)(S_2C_2Me_2)_2]^{1-}$ (M = Mo, W) were prepared as structural analogues of the reduced enzyme site. The systems, $[ML(S_2C_2Me_2)_2]^{1-}/SeO_4^{2-}$ (L = OMe, OPh, SC_6H_2-2,4,6-Pr^i_3) in acetonitrile, cleanly reduce selenate to selenite in second-order reactions whose negative entropies of activation implicate associative transition states. Rate constants at 298 K are in the 10^{-2}–10^{-4} M^{-1} s^{-1} range with $\Delta S^{\ddagger}$ = –12 to –34 eu. When rate constants are compared with previous data for the reduction of $(CH_2)_4SO$, Ph_3AsO, and nitrate by oxygen atom transfer, reactivity trends dependent on the metal, axial ligand L, and substrate are identified. As in all other cases of substrate reduction by oxo transfer, the kinetic metal effect $k_2^W > k_2^{Mo}$ holds. A proposal from primary sequence alignments suggesting that a conserved Asp residue is a likely ligand in the type II enzymes in the DMSO reductase family has been pursued by synthesis of the $[Mo^{IV}(O_2CR)(S_2C_2Me_2)_2]^{1-}$ (R = Ph, Bu^t) complexes. The species display symmetrical η^2-carboxylate binding and distorted trigonal prismatic stereochemistry. They serve as possible structural analogues of the reduced sites of nitrate, selenate, and perchlorate reductases under the proposed aspartate coordination. Carboxylate binding has been crystallographically demonstrated for one nitrate reductase, but not for the other two enzymes.

Introduction

Research in this laboratory on biomimetic molybdenum and tungsten chemistry[1] has resulted in the synthesis and characterization of active site structural analogues and the development of analogue reaction systems of members of the sulfite oxidase and DMSO reductase (DMSOR) enzyme families.[2] Square-pyramidal $[M^{IV}L(S_2C_2Me_2)_2]^{1-}$ and distorted octahedral $[M^{VI}OL(S_2C_2Me_2)_2]^{1-}$ complexes (M = Mo; L = RO^-, RS^-)[3–5] are accurate representations of the reduced and oxidized native enzyme sites, respectively, of the DMSOR family.[6] They also apply to at least one tungsten isoenzyme[7] and, potentially, to other tungstoenzyme sites (M = W; L = RO^-, RS^-, RCO_2^-).[8–11] Functional reaction systems capable of reducing biological *S*-oxide and *N*-oxide substrates[5,9,12] and nitrate[13] have been demonstrated using these molecules as stoichiometric reactants. These systems proceed by primary oxygen atom (oxo) transfer reactions[14] and display second-order kinetics that implicate associative transition states.

With results from the foregoing reaction systems in hand, we have turned our attention to other biological substrates to learn which of them can be transformed to the biological product by primary oxo transfer reactions. Among the enzymes of interest in this context are arsenite oxidase and selenate reductase.[15,16] We have recently reported oxo transfer reactions of the type $M^{IV} + As^{V}O \rightarrow M^{VI}O + As^{III}$ with M

* To whom correspondence should be addressed. E-mail: holm@chemistry.harvard.edu.

(1) Enemark, J. H.; Cooney, J. J. A.; Wang, J.-J.; Holm, R. H. *Chem. Rev.* **2004**, *104*, 1175–1200.
(2) Hille, R. *Chem. Rev.* **1996**, *96*, 2757–2816.
(3) Donahue, J. P.; Goldsmith, C. R.; Nadiminti, U.; Holm, R. H. *J. Am. Chem. Soc.* **1998**, *120*, 12869–12881.
(4) Lim, B. S.; Donahue, J. P.; Holm, R. H. *Inorg. Chem.* **2000**, *39*, 263–273.
(5) Lim, B. S.; Holm, R. H. *J. Am. Chem. Soc.* **2001**, *123*, 1920–1930.
(6) Kisker, C.; Schindelin, H.; Rees, D. C. *Annu. Rev. Biochem.* **1997**, *66*, 233–267.
(7) Garner, C. D.; Stewart, L. J. *Met. Ions Biol. Syst.* **2002**, *39*, 699–726.
(8) Sung, K.-M.; Holm, R. H. *Inorg. Chem.* **2000**, *39*, 1275–1281.
(9) Sung, K.-M.; Holm, R. H. *J. Am. Chem. Soc.* **2001**, *123*, 1931–1943.
(10) Sung, K.-M.; Holm, R. H. *Inorg. Chem.* **2001**, *40*, 4518–4525.
(11) Jiang, J.; Holm, R. H. *Inorg. Chem.* **2004**, *43*, 1302–1310.
(12) Sung, K.-M.; Holm, R. H. *J. Am. Chem. Soc.* **2002**, *124*, 4312–4320.
(13) Jiang, J.; Holm, R. H. *Inorg. Chem.* **2005**, *44*, 1068–1072.
(14) Holm, R. H. *Chem. Rev.* **1987**, *87*, 1401–1449.

10.1021/ic0521630 CCC: $33.50
Published on Web 03/10/2006

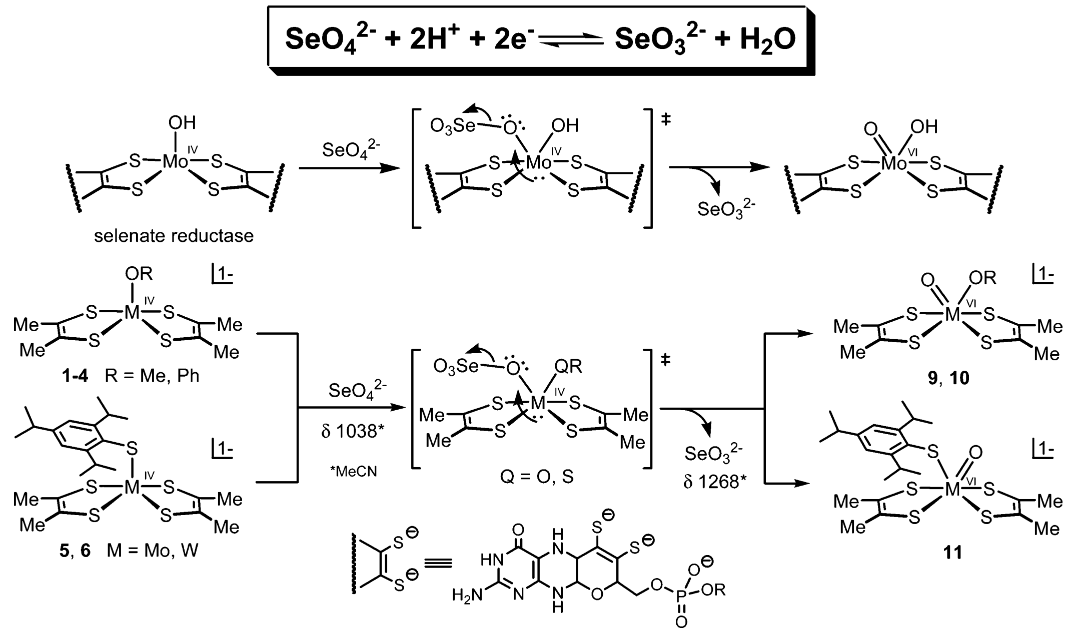

Figure 1. Depiction of the selenate reductase reaction based on the $\{Mo^{IV}(OH)(S_2pd)_2\}$ and $\{Mo^{VI}O(OH)(S_2pd)\}$ active site structures postulated from X-ray absorption spectroscopy, and that of analoguous reaction systems based on complexes of the general type $[M^{IV}(QR)(S_2C_2Me_2)_2]^{1-}$ (M = Mo, W; Q = O, S). Also included are likely formulations of the associative transition states, ^{77}Se chemical shifts, and the structure of the pyranopterindithiolene ligand dianion (S_2pd; R absent or contains a nucleotide, usually guanine).

= Mo and W.[17] Selenate reductase (SeR)[18] is a periplasmic molybdoenzyme that catalyzes the reaction in Figure 1. Selenate reduction to selenite has been associated with the respiratory electron-transfer chains of certain bacteria, including *T. selenatis*, whose SeR is the most thoroughly characterized. The enzyme has been crystallized,[19] but its full structure is not currently available. EXAFS analysis has led to the postulated active site structures in Figure 1.[20] The oxidized form reveals ~4 Mo−S interactions at 2.33 Å, one Mo═O bond at 1.68 Å, and one Mo−O bond at 1.81 Å. The reduced form shows ~4 Mo−S interactions at 2.32 Å and one or two Mo−O bonds at 2.22 Å. With recognition of the qualifications applied to these site formulations,[20] we have proceeded with them as guides for the correct structures of the two oxidation states and, thereafter, as reactant and product in potential oxo transfer reactions. Under the Hille classification,[2] the probable presence of two pyranopterindithiolene ligands places SeR, like arsenite oxidase with similar site structures,[21] in the DMSOR family. Within this family, the sites of these two enzymes differ from other members by apparently not involving protein ligands. We demonstrate in this investigation that selenate is reducible to selenite by molybdenum- and tungsten-mediated oxo transfer reactions.

(15) Schröder, I.; Rech, S.; Krafft, T.; Macy, J. M. *J. Biol. Chem.* **1997**, *272*, 23765−23768.
(16) Watts, C. A.; Ridley, H.; Dridge, E. J.; Leaver, J. T.; Reilly, A. J.; Richardson, D. J.; Butler, C. S. *Biochem. Soc. Trans.* **2005**, *33*, 173−175.
(17) Wang, J.-J.; Kryatova, O.; Rybak-Akimova, E. V.; Holm, R. H. *Inorg. Chem.* **2004**, *43*, 8092−8101.
(18) Abbreviations are given in the chart.
(19) Maher, M. J.; Macy, J. M. *Acta Crystallogr.* **2002**, *D58*, 706−708.
(20) Maher, M. J.; Santini, J.; Pickering, I. J.; Prince, R. C.; Macy, J. M.; George, G. N. *Inorg. Chem.* **2004**, *43*, 402−404.
(21) Conrads, T.; Hemann, C.; George, G. N.; Pickering, I. J.; Prince, R. C.; Hille, R. *J. Am. Chem. Soc.* **2002**, *124*, 11276−11277.

Experimental Section

Preparation of Compounds. All reactions and manipulations were performed under a pure dinitrogen atmosphere using either an inert atmosphere box or standard Schlenk techniques.

Methanol was distilled from magnesium; acetonitrile, ether, dichloromethane, and THF were freshly purified using an Innovative Technology solvent purification system and stored over 4-Å molecular sieves. The compounds Na_2SeO_3, Na_2SeO_4, Ph_3AsO, and $(CH_2)_4SO$ (distilled over molecular sieves) were commercial samples (Aldrich). The compounds $(Et_4N)(RCO_2)$ (R = Bu^t, Ph) were prepared by equimolar reaction of RCO_2H and 25% Et_4NOH in methanol and obtained as colorless crystalline solids after recrystallization from acetonitrile/ether. The Et_4N^+ salts of $[M(OPh)(S_2C_2Me_2)_2]^{1-}$ (M = Mo,[5] W[8]) and $[M(SC_6H_2\text{-}2,4,6\text{-}Pr^i_3)(S_2C_2Me_2)_2]^{1-}$ (M = Mo,[4] W[11]) were prepared as described. In the following preparations, all volume reduction and evaporation steps were performed in vacuo.

$(Et_4N)_2[SeO_4]$. Reactions were performed in subdued light. To a solution of 3.74 g (20.0 mmol) of Na_2SeO_4 in 30 mL of water was added a solution of 6.90 g (40.6 mmol) of $AgNO_3$ in 40 mL of water. The reaction mixture was stirred for 1 h, and the white solid was collected, washed with water, methanol, and ether to yield 6.60 g (92%) of Ag_2SeO_4. A mixture of 2.50 g (7.00 mmol) of Ag_2SeO_4 and 2.09 g (10.0 mmol) of Et_4NBr was treated with 150 mL of methanol. The reaction mixture was stirred for 24 h and filtered, and the filtrate taken to dryness.

The solid was washed with water, methanol, and ether to give the product as 1.76 g (87%) of a white solid, which upon recrystallization from acetonitrile/hexane was obtained as colorless rectangular crystals. ^{77}Se NMR (MeCN): δ 1038.

$(Et_4N)[HSeO_3]$. The previous preparation was followed using Na_2SeO_3 instead of Na_2SeO_4. The product was isolated as colorless blocklike crystals (85%) after recrystallization from acetonitrile/hexane and was identified as the hydrogenselenite salt by an X-ray structure determination. ^{77}Se NMR (MeCN): δ 1360.

$(Et_4N)[W(OMe)(S_2C_2Me_2)_2]$. Method A. To a frozen solution of 120 mg (0.25 mmol) of $[W(CO)_2(S_2C_2Me_2)_2]$[22,23] in 2 mL of THF in a dry ice-acetone bath was added a suspension of 13.5 mg (0.25 mmol) of NaOMe in 0.25 mL of acetonitrile. The frozen mixture was allowed to warm to −20 °C, resulting in a color change from reddish-violet to bluish-violet. The reaction solution was treated with a solution of 42 mg (0.25 mmol) of Et_4NCl in 1 mL of acetonitrile at −20 °C and stirred for 5 min. The dark violet solid obtained after solvent removal was washed with ether (3 × 5 mL, −20 °C) and dissolved in 1.5 mL of acetonitrile, and the solution was filtered. The filtrate was allowed to stand at −20 °C for 2 d, during which a mixture of large brown blocklike crystals and a much smaller amount of violet needle-shaped crystals formed. The brown crystals were mechanically separated, washed with ether (3 × 5 mL, −20 °C), and dissolved in 1 mL of acetonitrile. Ether (20 mL) was layered on the solution, which was allowed to stand for 2 d. The product was obtained as 73 mg (50%) of large brown crystals. ^1H NMR (CD_3CN, anion): δ 2.57 (s, 4), 3.47 (s, 1). Absorption spectrum (acetonitrile): λ_{max} (ϵ_M) 287 (11300), 312 (9800), 385 (sh, 1600), 426 (900), 551 (800) nm. Anal. Calcd for $C_{17}H_{35}NOS_4W$: C, 35.11; H, 6.07; N, 2.41; S, 22.01. Found: C, 34.98; H, 5.96; N, 2.34; S, 22.16.

Method B. All steps were carried out at −20 °C. A solid mixture of 120 mg (0.25 mmol) of $[W(CO)_2(S_2C_2Me_2)_2]$, 13.5 mg (0.25 mmol) of NaOMe, and 42 mg (0.25 mmol) of Et_4NCl was dissolved in a minimal volume (ca. 2 mL) of acetonitrile/THF (1:1 v/v). The bluish-violet solution that formed within 1 min was stirred for 20 min. Ether (40 mL) was layered on the solution. The product was obtained upon standing for 2 d, followed by the separation of crystals as in method A, as 78 mg (54%) of brown crystals. Spectral properties are the same as those of the product obtained by Method A.

$(Et_4N)[Mo(OMe)(S_2C_2Me_2)_2]$. This compound was prepared by procedures analogous to those for $(Et_4N)[W(OMe)(S_2C_2Me_2)_2]$ with $[Mo(CO)_2(S_2C_2Me_2)_2]$[4,22] and was isolated as orange-brown blocklike crystals (40%). ^1H NMR (CD_3CN, anion): δ 2.50 (s, 4), 3.42 (s, 1). Absorption spectrum (acetonitrile): λ_{max} (ϵ_M) 325 (9700), 388 (sh, 4300), 458 (sh, 1800), 550 (sh, 960), 728 (400) nm. This compound was identified by an X-ray structure determination.

$(Et_4N)[WO(OMe)(S_2C_2Me_2)_2]$. The procedure is similar to that for compounds of the type $(Et_4N)[WO(OR)(S_2C_2Me_2)_2]$.[8,9] To a frozen orange-brown solution of 116 mg (0.20 mmol) of (Et_4N)-$[W(OMe)(S_2C_2Me_2)_2]$ in 2.5 mL of acetonitrile in a dry ice-acetone bath was injected a solution of 18.0 mg (0.24 mmol) of Me_3NO in 0.2 mL of acetonitrile. The frozen mixture was warmed to room temperature over 20 min, resulting in a color change to greenish-brown. The solution was layered with 40 mL of cold ether and maintained at −20 °C over 2 d. The solid obtained by decantation of the pale greenish-brown supernatant was washed with cold ether (−20 °C, 3 × 5 mL) and dried to yield the product as 92.0 mg (77%) of a brown-black crystalline solid. ^1H NMR (CD_3CN, anion): δ 2.17 (s, 4), 4.08 (s, 1). IR (KBr): ν_{WO} 891 cm^{-1}. Absorption spectrum (acetonitrile): λ_{max} (ϵ_M) 330 (6500), 477 (4500), 625 (3000) nm. Anal. Calcd for $C_{17}H_{35}NO_2S_4W$: C, 34.17; H, 5.91; N, 2.35; S, 21.42. Found: C, 34.30; H, 6.03; N, 2.40; S, 21.58.

$(Et_4N)[Mo(O_2CBu^t)(S_2C_2Me_2)_2]$. To a violet solution of 77.7 mg (0.20 mmol) of $[Mo(CO)_2(S_2C_2Me_2)_2]$ in 2 mL of THF was added a solution of 46.2 mg (0.20 mmol) of $(Et_4N)(O_2CBu^t)$ in 2 mL of acetonitrile. The reaction mixture became orange-red immediately, was stirred for 30 min, and was filtered. The filtrate was layered with 25 mL of ether. The solid that separated was washed with ether (3 × 3 mL) and dried to produce 77 mg (68%) of a red-brown microcrystalline product. ^1H NMR (CD_3CN, anion): δ 0.84 (s, 4), 2.65 (s, 3). IR (KBr): ν_{COO} 1438 cm^{-1}. Absorption spectrum (acetonitrile): λ_{max} (ϵ_M) 270 (4800), 328 (1850), 379 (sh, 1700), 409 (2300), 491 (1850), 734 (200) nm. Anal. Calcd for $C_{21}H_{41}NMoO_2S_4$: C, 44.75; H, 7.34; N, 2.49; S, 22.71. Found: C, 44.85; H, 7.28; N, 2.43; S, 22.68.

Chart 1

$[M^{IV}(OMe)(S_2C_2Me_2)_2]^{1-}$	M = Mo **1**, W **2**
$[M^{IV}(OPh)(S_2C_2Me_2)_2]^{1-}$	M = Mo **3**[5], W **4**[8]
$[M^{IV}(SC_6H_2\text{-}2,4,6\text{-}Pr^i_3)(S_2C_2Me_2)_2]^{1-}$	M = Mo **5**[4], W **6**[11]
$[Mo^{IV}(O_2CR)(S_2C_2Me_2)_2]^{1-}$	R = Bu^t **7**, Ph **8**
$[W^{VI}OL(S_2C_2Me_2)_2]^{1-}$	L = OMe **9**, OPh **10**[9]
	L = $SC_6H_2\text{-}2,4,6\text{-}Pr^i_3$ **11**[11]
$[Mo_2O(S_2C_2Me_2)_4]^{1-}$	**12**
$[W^{VI}O(O_2CPh)(S_2C_2Me_2)_2]^{1-}$	**13**[11]
$[W^{IV}O(S_2C_2Me_2)_2]^{2-}$	**14**[23]

DMSO, DMSO reductase; Nar, membrane-bound nitrate reductase; R*, $C_6H_2\text{-}2,4,6\text{-}Pr^i_3$; S_2pd, pyranopterindithiolene(2−) cofactor ligand; SeR, selenate reductase; XAS, x-ray absorption spectroscopy.

$(Et_4N)[Mo(O_2CPh)(S_2C_2Me_2)_2]$. To a mixture of 77.7 mg (0.20 mmol) of $[Mo(CO)_2(S_2C_2Me_2)_2]$ and 50.2 mg (0.20 mmol) of $(Et_4N)(O_2CPh)$ was added 4 mL of THF and 1 mL of acetonitrile. The orange-red solution that formed immediately was stirred for 1 h, resulting in a precipitate, which was collected and washed with ether/THF (2:1 v/v, 3 × 3 mL) and ether (3 × 3 mL) to give the product as 80 mg (69%) of an orange-red solid. ^1H NMR (CD_3CN, anion): δ 2.69 (s, 12), 7.34 (t, 2), 7.51 (t, 1), 7.69 (d, 2). IR (KBr): ν_{COO} 1442 cm^{-1}. Absorption spectrum (acetonitrile): λ_{max} (ϵ_M) 272 (6200), 331 (27000), 370 (2800), 416 (3350), 497 (2700) nm. Anal. Calcd. for $C_{23}H_{37}MoNO_2S_4$: C, 47.33; H, 6.40; N, 2.40; S, 21.93. Found: C, 47.19; H, 6.40; N, 2.40; S, 21.91.

In the following sections, complexes **1**−**14** are designated as in Chart 1.

X-ray Structure Determinations. The structures of the eight compounds in Table 1 were determined. Suitable crystals were obtained by layering several volume equivalents of ether on acetonitrile solutions which were maintained at 273 K for at least 12 h. Crystals were coated in paratone-N oil and mounted on either a Bruker SMART 1K or APEX CCD-based diffractometer equipped with an LT-2 low-temperature apparatus operating at 213 K. Data were collected with ω scans of 0.3°/frame for 30 s (60 s for **7** and **8**), so that 971−1647 frames were collected for a hemisphere of data. The first 50 frames were recollected at the end of the data collection to monitor for decay; no significant decay was detected for any compound. Cell parameters were retrieved using SMART software and refined using SAINT software on all reflections. Data integration was performed with SAINT, which corrects for Lorentz polarization and decay. Absorption corrections were applied using SADABS. Space groups were assigned unambiguously by analysis of symmetry and systematic absences determined by XPREP. The compound (Et_4N)[**1**] occurred as a twinned crystal, as determined by the TwinRotMax routine in PLATON and confirmed by ROTAX software. A 2-fold axis along the −1 0 1 reciprocal lattice direction was observed. The data were detwinned by incorporation of TWIN instruction in SHELXTL with the matrix 0 0 −1, 0 −1 0, −1 0 0. The compound (Et_4N)[**7**] was at first unsuccessfully refined using a unit cell 4× smaller (a = 9.449 Å, b = 16.399 Å, c = 17.678 Å;

(22) Fomitchev, D. V.; Lim, B. S.; Holm, R. H. *Inorg. Chem.* **2001**, *40*, 645−654.
(23) Goddard, C. A.; Holm, R. H. *Inorg. Chem.* **1999**, *38*, 5389−5398.

Table 1. Crystallographic Data

	(Et_4N)[**1**]	(Et_4N)[**2**]	(Et_4N)[**7**]	(Et_4N)[**8**]	(Et_4N)[**9**]	(Et_4N)[**12**] ·MeCN	$[Et_4N]_2[SeO_4]$ ·MeCN	$[Et_4N][HSeO_3]$
formula	$C_{17}H_{35}MoNOS_4$	$C_{17}H_{35}NOS_4W$	$C_{21}H_{41}MoNO_2S_4$	$C_{23}H_{37}MoNO_2S_4$	$C_{17}H_{35}NO_2S_4W$	$C_{26}H_{47}Mo_2N_2OS_8$	$C_{18}H_{43}N_3O_4Se$	$C_8H_{21}NO_3Se$
fw	493.64	581.55	563.73	583.72	597.55	852.02	444.51	258.22
space group	$P2_1/n$	$P2_1/c$	$Pca2_1$	$P2_1/n$	$P2_1/n$	$P2_1/c$	$P2_1/n$	$P\bar{1}$
Z	8	4	16	4	4	4	4	2
a (Å)	22.978(8)	10.118(2)	37.741(11)	8.919(2)	8.979(3)	18.158(2)	13.182(7)	7.926(6)
b (Å)	9.645(3)	11.058(2)	16.381(5)	23.807(4)	16.925(5)	11.582(2)	14.176(7)	8.909(7)
c (Å)	22.968(8)	21.161(4)	17.663(5)	12.949(3)	15.476(5)	18.029(2)	13.370(7)	9.146(7)
α (deg)								80.64(1)
β (deg)	109.56(1)	97.029(3)		105.303(4)	91.944(5)	104.997(2)	114.35(2)	65.15(1)
γ (deg)								77.19(2)
V (Å^3)	4797(3)	2349.8(8)	10920(6)	2652.0(10)	2350.5(13)	3662.4(8)	2276(2)	569.7(8)
d_{calcd} (g/cm^3)	1.367	1.644	1.372	1.462	1.689	1.545	1.297	1.505
μ^a (mm^{-1})	0.900	5.277	0.803	0.830	5.281	1.164	1.675	3.276
θ range (deg)	0.94−25.00	1.94−25.00	1.08−25.00	1.71−26.00	1.78−27.86	1.16−26.00	1.83−27.88	2.35−28.05
GOF (F^2)	1.052	1.050	1.209	1.095	1.255	1.032	1.052	1.060
R1,^{b} %	6.86	4.04	7.34	3.96	3.60	2.96	3.33	3.76
wR2,^{c} %	14.50	10.09	14.25	9.21	8.39	6.89	8.34	9.45

^{a} Mo Kα radiation. ^{b} $R1 = \sum||F_o| - |F_c||/\sum|F_o|$. ^{c} $wR2 = \{\sum[w(F_o^2 - F_c^2)^2]/\sum[w(F_o^2)^2]\}^{1/2}$

*Pna*2$_1$ or *Pnma*) that was found by the matrix routine in SMART. Very large thermal parameters, as well as strong residual electron density, were observed. Upon careful examination of the collected frames, weak reflections not accounted for in the unit cell determination were observed and included in the cell index routine in SMART to generate the unit cell parameters in Table 1. Missing symmetry in all crystals was checked with PLATON; none was found. Structures were solved by direct methods and refined against all data by full-matrix least-squares techniques on F^2 using the SHELXL-97 package. All non-hydrogen atoms were refined anisotropically. Hydrogen atoms were placed at idealized positions on carbon atoms. Crystal parameters and agreement factors are reported in Table 1.[24]

Kinetics Measurements. All reactions were performed under strictly anaerobic conditions in acetonitrile (Burdick & Jackson) which was stored over 4 Å molecular sieves prior to use. Oxo transfer reactions were monitored with a Varian Cary 3 spectrophotometer equipped with a cell compartment thermostated to ±0.5 °C and a multicell changer. Thermal equilibrium was reached by placing a 1 mm quartz cell containing 0.24−0.32 mL of the solution of the complex in the cell compartment at least 5 min prior to the start of a reaction. Reactions were initiated upon injection of the substrate solution containing oxo donor XO by means of a gastight syringe through the rubber septum cap of the cell followed by rapid shaking of the reaction mixture. Reaction systems contained the initial concentrations [**1**−**6**]$_0$ = 1.37−2.14 mM, $[SeO_4^{2-}]_0$ = 11.1−29.4 mM, $[(CH_2)_4SO]_0$ = 1.59−3.27 M, and $[Ph_3AsO]_0$ = 3.8−11.3 mM. Sharp isosbestic points were observed for each reaction system, indicating the lack of detectable intermediates. For each substrate, reactions were conducted at five temperatures in the 278−333 K range. At each temperature, at least five independent runs with different initial concentrations of XO were performed under pseudo-first-order conditions. Plots of k_{obs} versus $[XO]_0$ were linear and yielded overall second-order rate constants, k_2, at each temperature. Final values of k_2 were averages from multiple independent runs. Activation parameters were determined from Eyring plots of k_2 versus $(k_BT/h)[\exp(\Delta S^‡/R - \Delta H^‡/RT)]$. Standard deviations were estimated using linear least-squares error analysis with uniform weighting of the data points.

Other Physical Measurements. All measurements were made under anaerobic conditions. NMR spectra were recorded on Varian Mercury 400 and 300 spectrometers. Chemical shifts of $^{77}Se\{^1H\}$ spectra are referenced to Me_2Se. Infrared spectra were determined with a Nicolet Nexus 470 FT-IR instrument. Absorption spectra were obtained with a Varian Cary 50 Bio spectrophotometer.

(24) See paragraph at the end of this article for Supporting Information.

Results and Discussion

Reaction Systems. From the reduced des-oxo SeR site structure in Figure 1, a desirable molybdenum reactant in substrate reduction by oxo transfer is a bis(dithiolene)Mo^{IV}-(OH) complex. Hydrolysis of the complexes $[M(OPh)(S_2C_2Me_2)_2]^{1-}$ (M = Mo, W) in aqueous acetonitrile media yields $[MO(S_2C_2Me_2)_2]^{2-}$.[5,9] While a hydroxo species is a likely intermediate in these reactions, no M^{IV}−OH dithiolene complexes have been isolated or otherwise identified in these or other systems. In the absence of hydroxo species, we have utilized the methoxide complexes **1** and **2** whose preparation is outlined in Figure 2. Here methoxide is the closest available simulator of hydroxide provided that SeR is an oxotransferase. Note that the enzyme is a reductase, not a hydroxylase which utilizes bound hydroxide as a nucleophile in oxidase reactions.[25] We have also utilized phenolate complexes **3** and **4** as additional reactants with axial anionic oxygen ligands and for comparison with previous kinetics results. Thiolate complexes **5** and **6** are structural analogues of the reduced sites of nitrate reductase with axial cysteinate ligation[26] and relate the present work to our recent study of nitrate reduction.[13] Although SeR is not known to be a tungstoenzyme, we have included W^{IV} reactants to provide additional examples of the kinetic metal effect and to otherwise follow our past practice of elaborating in parallel the chemistry of analogous molybdenum and tungsten systems. The stable W^{VI}O complex **9** when detected in an oxo transfer reaction demonstrates the fate of the oxygen atom transferred from substrate. This compound has been isolated and structurally characterized. Corresponding com-

(25) Hille, R. *Arch. Biochem. Biophys.* **2005**, *433*, 107−116.
(26) Dias, J. M.; Than, M. E.; Humm, A.; Huber, R.; Bourenkov, G. P.; Bartunik, H. D.; Bursakov, S.; Calvete, J.; Caldeira, J.; Carneiro, C.; Moura, J. J. G.; Moura, I.; Romão, M. J. *Structure* **1999**, *7*, 65−79.

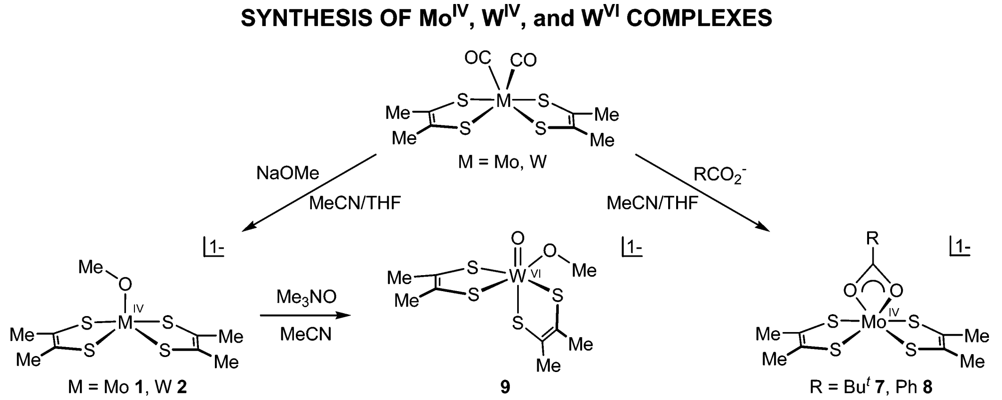

Figure 2. Scheme for the synthesis of the complexes $[M(OMe)(S_2C_2Me_2)_2]^{1-}$, $[Mo(O_2R)(S_2C_2Me_2)_2]^{1-}$, and $[WO(OMe)(S_2C_2Me_2)_2]^{1-}$.

plexes of the type $[MoO(OR)(S_2C_2Me_2)_2]^{1-}$, while sometimes detectable in solution, are unstable because of autoreduction to $[Mo^VO(S_2C_2Me_2)_2]^{1-}$.[5]

Selenate was utilized as anhydrous $(Et_4N)_2[SeO_4]$, which is freely soluble in acetonitrile. This compound was prepared in high yield by simple metathesis reactions. The Me_4N^+ salt has been obtained by an ion-exchange procedure.[27] When Na_2SeO_3 was used in the metathesis reactions, the only product isolated was the hydrogenselenite compound $(Et_4N)[HSeO_3]$, a probable consequence of the greater basicity of selenite versus selenate (pK_a = 6.58 for $HSeO_3^-$, 2.05 for $HSeO_4^-$).

Structural Features. While crystals containing complexes **1** and **2** with the same cation would be expected to be isomorphous, as is the case with, for example, the Et_4N^+ salts of **8** and $[W(O_2CPh)(S_2C_2Me_2)_2]^{1-}$,[10] different packing patterns are found. This behavior has been observed previously with the Et_4N^+ salts of **3**[5] and **4**.[8] The structure of **2**, provided in Figure 3, reveals these essential features: square pyramidal geometry with the metal atom displaced 0.75 Å above the S_4 mean plane toward the axial methoxide ligand, a trans S−W−S angle of 142.6(7)° and a dihedral angle of 129.6° between the chelate ring planes. For isostructural Mo^{IV} complex **1** (not shown), the mean Mo−S distance of 2.33(1) Å agrees very well with the 2.32 Å value from the EXAFS analysis of the reduced enzyme. The mean Mo−O distance of 1.862(3) Å differs largely from the value of 2.22 Å from the EXAFS investigation, where the identification of oxygen ligands is described as tentative because of the correlation with intense Mo−S scattering.[20] The values for **1** are averaged over two crystallographically independent anions; this complex is practically isometric with **2**.[24] For **2**, the W−O bond length is 1.824(5) Å. Recent geometry-optimized DFT calculations of $[M(OMe)(S_2C_2H_2)_2]^{1-}$ place the M−OMe bond length at 1.887 Å (Mo) and 1.874 Å (W).[28] Consequently, an authentic M−OH distance in the enzyme site is expected to lie in the 1.8−1.9 Å range and is found without exception for M^{IV}−OR bonds in these and other bis(dithiolene) complexes by crystallography[4,5,8,9] and XAS.[29,30] The long M−O interaction in the enzyme is presumably the basis for the des-oxo designation.[20]

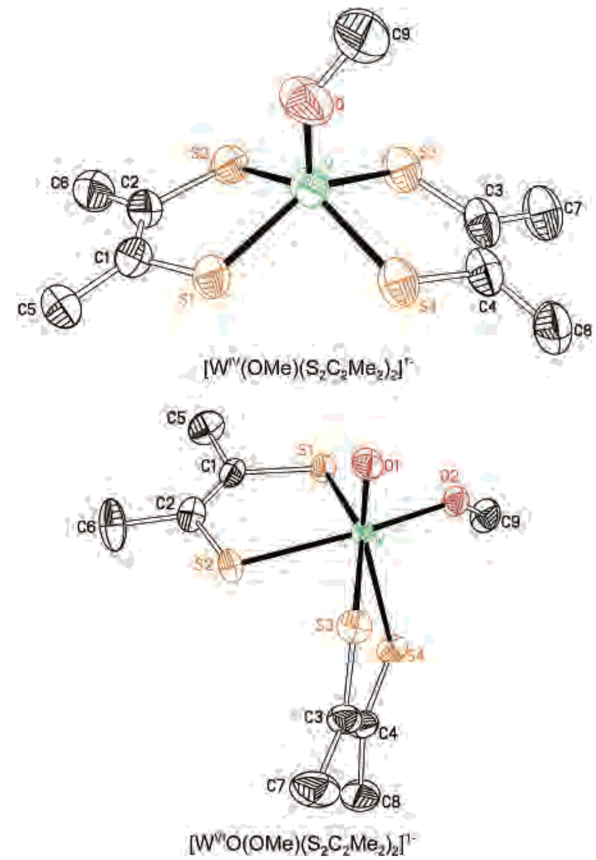

Figure 3. Structures of tungsten complexes showing 50% probability ellipsoids and atom labeling schemes. Selected (mean) bond distances (Å) and angles (deg) for $[W(OMe)(S_2C_2Me_2)_2]^{1-}$ (upper): W−O = 1.824(5), W−S = 2.33(1), S−C = 1.778(5), C−C = 1.323(5), S1−W−S2 = 81.91(6), S3−W−S4 = 82.51(7), O−W−S = 107.9(3)−109.4(2), δ = 0.746(1), θ = 129.6(1). For $[WO(OMe)(S_2C_2Me_2)_2]^{1-}$ (lower): W−O1 = 1.724(4), W−O2 = 1.926(4), W−S1,2,3 = 2.40(1), W−S4 = 2.523(2), O1−W−O2 = 93.8(2), S1−W−S2 = 79.53(5), S3−W−S4 = 78.17(5), S2−W−S4 = 89.61(5), S1−W−S3 = 157.05(5), θ = 91.3(1). All but the last two S−W−S angles are chelate ring bite angles.

Structures of the substrate selenate ion and of the hydrogenselenite ion are shown in Figure 4. These structures were

(27) Malchus, M.; Jansen, M. *Z. Naturforsch.* **1998**, *53b*, 704−710.
(28) McNamara, J. P.; Hillier, I. H.; Bhachu, T. S.; Garner, C. D. *Dalton Trans.* **2005**, 3572−3579.
(29) Musgrave, K. B.; Donahue, J. P.; Lorber, C.; Holm, R. H.; Hedman, B.; Hodgson, K. O. *J. Am. Chem. Soc.* **1999**, *121*, 10297−10307.
(30) Musgrave, K. B.; Lim, B. S.; Sung, K.-M.; Holm, R. H.; Hedman, B.; Hodgson, K. O. *Inorg. Chem.* **2000**, *39*, 5238−5247.

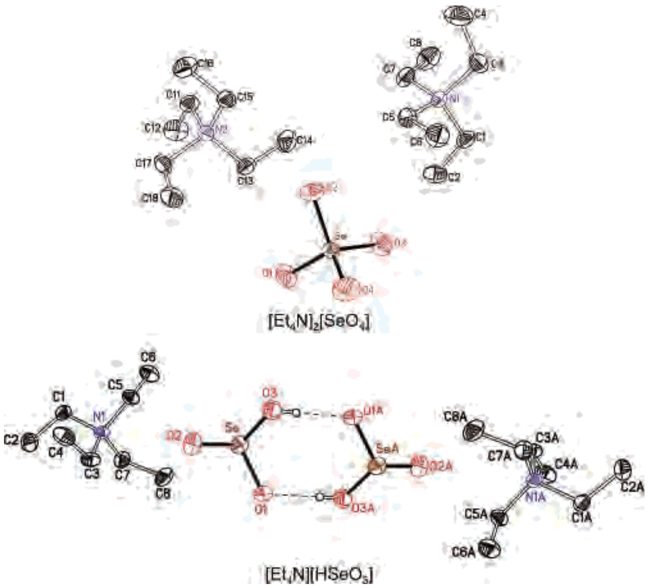

Figure 4. Structures of $(Et_4N)_2[SeO_4]$ and $(Et_4N)[HSeO_3]$. In the latter, the hydrogen bonding pattern to a symmetry equivalent molecule A is shown. Selected (mean) bond distances and angles: for $[SeO_4]^{2-}$ Se−O = 1.641(3), O−SeO = 109.5(2); for $[HSO_3]^-$ Se−O1 = 1.678(2), Se−O2 = 1.639(2), Se−O3 = 1.758(2), O1···O3A = 2.691(3), O1−Se−O2 = 107.1(1), O1−Se−O3 = 101.3(1), O2−Se−O3 = 99.9(1).

used to identify the compounds and demonstrate the absence of water or other protic solvates in the crystals. The tetrahedral structure of SeO_4^{2-} in the monoclinic Et_4N^+ salt acetonitrile monosolvate displays angles and distances indistinguishable from those of cubic $(Me_4N)_2[SeO_4]$[27] and $Li_2SeO_4{\cdot}H_2O$.[31] The close O3···O1 contact (2.691(3) Å) in the Et_4N^+ salt of $HSeO_3^-$ indicates the presence of hydrogen bonding. A hydrogen atom was placed on atom O3 with Se−O3 = 1.758(2) Å, and its position was constrained in the O3···O1 direction, resulting in an O1A···H3 bond distance of 1.88 Å. Prior structures of hydrogenselenite compounds with organic counterions reveal hydrogen bonding between the anion and cation and a pattern of Se−O distances similar to that found here.[32−35] None of these structures contain mutually hydrogen-bonded hydrogenselenite anions.

The product complex derived from **2** by oxo transfer is $W^{VI}O$ complex **9**, whose structure is found in Figure 3. Its principal features are a cis disposition of the oxo and methoxide ligands, a dihedral angle, θ, of 91.3° between chelate rings, a pronounced trans effect of the oxo ligand causing the W−S4 bond to be 0.11−0.13 Å longer than the other three W−S distances, and a trans ligand angle, S1−W−S3, of 157.1°. This angle describes a structure intermediate between the octahedral (180°) and trigonal prismatic (136°) limits.[36] The structure of **9** is closely

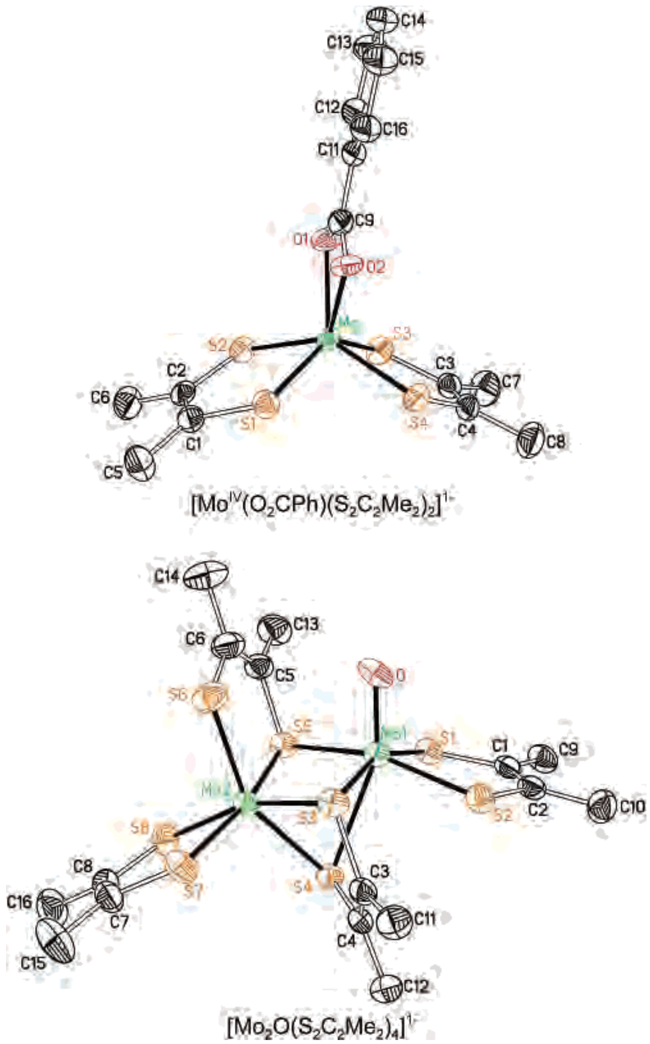

Figure 5. Structures of $[Mo(O_2CPh)(S_2C_2Me_2)_2]^{1-}$ and $[Mo_2O(S_2C_2Me_2)_4]^{1-}$ showing 50% probability ellipsoids and atom labeling schemes.

comparable to those of **10**[9] and **11**,[11] which are also oxo transfer products.

In the course of preparing methoxide complexes **1** and **2**, bluish-violet reaction mixtures were always observed, and a small amount of violet byproduct was encountered when isolating the desired brown product compounds. Because of its persistent appearance, the purple crystals obtained in the preparation of **1** were crystallographically examined. This material was shown to be (Et_4N)[**12**], containing a mixed-valence binuclear complex whose structure is included in Figure 5. It is formally (but not uniquely) an addition product of $[Mo(S_2C_2Me_2)_3]^{1-}$, a known compound[4] which we have often encountered as an impurity in the synthesis of other molybdenum dithiolenes, and the neutral fragment $[MoO(S_2C_2Me_2)]$. The origin of the oxo ligand has not been established. Metric features are available elsewhere.[24]

Reduction of Selenate by Oxo Transfer. The reaction systems utilizing M^{IV} complexes **1**−**6** are depicted in Figure 1. The overall process is reaction 1, resulting in the formation of $M^{VI}O$ products and selenite. Of the former, only $W^{VI}O$

(31) Johnston, M. G.; Harrison, W. T. A. *Acta Crystallogr.* **2003**, *E59*, i25−i27.
(32) Ritchie, L. K.; Harrison, W. T. A. *Acta Crystallogr.* **2003**, *E59*, o1296−o1298.
(33) Nemec, I.; Chudoba, V.; Havlicek, D.; Cisarová, I.; Micka, Z. *J. Solid State Chem.* **2001**, *161*, 312−318.
(34) de Matos Gomes, E.; Nogueria, E.; Fernandes, I.; Belsley, M.; Paixâo, J. A.; Matos Beja, A.; Ramos Silva, M.; Martín-Gil, J.; Martín-Gil, F.; Mano, J. F. *Acta Crystallogr.* **2001**, *B57*, 828−832.
(35) Nêmec, I.; Cisarová, I.; Micka, Z. *J. Solid State Chem.* **1998**, *140*, 71−82.
(36) Beswick, C. L.; Schulman, J. M.; Stiefel, E. I. *Prog. Inorg. Chem.* **2004**, *52*, 55−110.

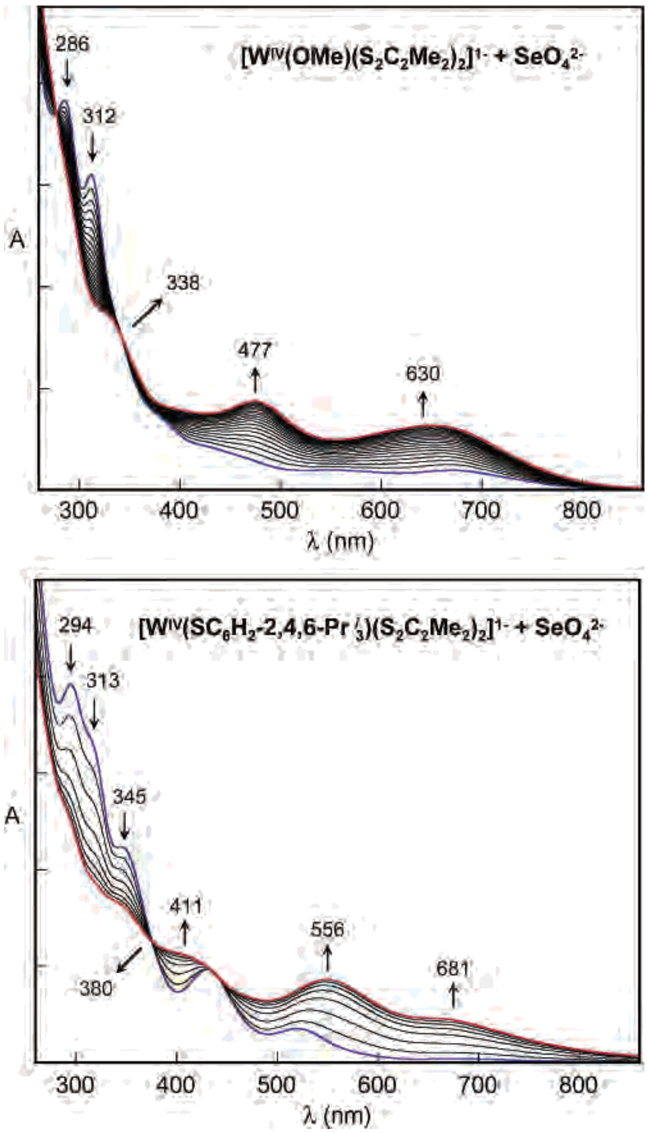

Figure 6. Spectrophotometric monitoring of reactions: (upper) the system $[W(OMe)(S_2C_2Me_2)_2]^{1-}/SeO_4^{2-}$ with $[\mathbf{2}]_0 = 1.48$ mM, $[SeO_4^{2-}]_0 = 14.3$ mM, and spectra recorded every 5 min; (lower) the system $[W(SC_6H_2\text{-}2,4,6\text{-}Pr^i{}_3)(S_2C_2Me_2)_2]^{1-}/SeO_4^{2-}$ with $[\mathbf{6}]_0 = 1.51$ mM, $[SeO_4^{2-}]_0 = 14.3$ mM, and spectra recorded every 3 min. Reactions were conducted in acetonitrile solutions at 298 K. Arrows indicate changes in absorbance with time; band maxima and isosbestic points are indicated.

complexes **9**−**11** are stable to isolation. Reaction 1 is an example of the generalized oxo transfer paradigm 2. The corresponding $Mo^{VI}O$ complexes are formed in reaction 1 but, as noted above, are not stable. Reactions were monitored spectrophotometrically, and data were analyzed as in previous work.[5,9,13,17] Illustrative spectra are shown for the systems based on complexes **2** and **6** in Figure 6. These and other reaction systems develop tight isosbestic points and proceed

$$[M^{IV}L(S_2C_2Me_2)_2]^{1-} + SeO_4^{2-} \rightarrow [M^{VI}OL(S_2C_2Me_2)_2]^{1-} + SeO_3^{2-} \quad (1)$$

$$M^{IV} + XO \rightarrow M^{VI} + X \quad (2)$$

$$-d[M^{IV}]/dt = k_2[M^{IV}][XO] \quad (3)$$

cleanly to completion. The exception is the reaction based on **1** whose spectra did not show clean isosbestic points; the kinetics of this system were not pursued. For the systems in Figure 6, the final spectra are identical to the spectra of authentic complexes **9** and **11**. The formation of these products can also be established by the characteristic methyl chemical shifts of $W^{VI}O$ complexes (δ 2.1−2.3 in acetonitrile). The formation of selenite is readily demonstrated by ^{77}Se NMR spectra. For example, in the reaction based on tungsten complex **6**, the spectrum in Figure 7 reveals the signal of substrate SeO_4^{2-} at δ 1038 and product SeO_3^{2-} at δ 1268. The product is not $HSeO_3^-$, which occurs at δ 1360. The values for selenate and selenite are very close to reported values in aqueous solution.[37]

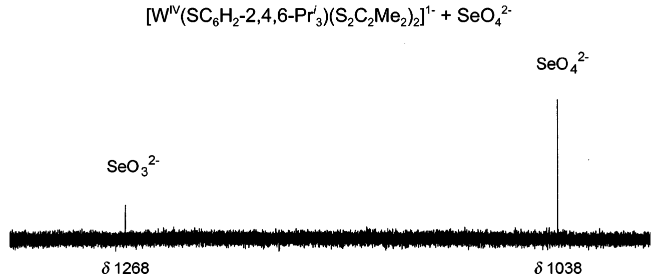

Figure 7. ^{77}Se NMR spectrum for the system $[W(SC_6H_2\text{-}2,4,6\text{-}Pr^i{}_3)(S_2C_2Me_2)_2]^{1-}/SeO_4^{2-}$ starting with 1 equiv of **6** and 4 equiv of SeO_4^{2-} after 1 h in acetonitrile solution at ambient temperature.

Table 2. Kinetics Parameters for Oxygen Atom Transfer Reactions in Selected Systems $[M^{IV}(QR)(S_2C_2Me_2)_2]^{1-}/XO$ in Acetonitrile at 298 K

M	QR	XO	k_2 (M^{-1} s^{-1})[j]	$\Delta H^{\ddagger}$ (kcal/mol)	$\Delta S^{\ddagger}$ (eu)
Mo[d]	OPh	SeO_4^{2-}	$7.2(4) \times 10^{-4}$	12(1)	−34(3)
Mo[e]	$SC_6H_2Pr^i{}_3$	SeO_4^{2-}	$3.2(2) \times 10^{-3}$	14.8(6)	−20(2)
W[g]	OMe	SeO_4^{2-}	$1.4(2) \times 10^{-3}$	12.2(4)	−30(1)
W[d,g]	OPh	SeO_4^{2-}	$3.3(3) \times 10^{-3}$	12.8(6)	−28(2)
W[e]	$SC_6H_2Pr^i{}_3$[d]	SeO_4^{2-}	3.6×10^{-2}	15.8(7)	−12(2)
W[a]	$SC_6H_2Pr^i{}_3$	NO_3^-	$1.7(1) \times 10^{-1}$	12.6(9)	−20(3)
Mo[b,f]	OPh	$(CH_2)_4SO$	$1.5(2) \times 10^{-4}$	10.1(4)	−39(1)
Mo[a]	$SC_6H_2Pr^i{}_3$	$(CH_2)_4SO$	$1.4(1) \times 10^{-3}$	16.8(6)	−16(2)
W[h]	OMe	$(CH_2)_4SO$	$8.5(1) \times 10^{-5}$	12.0(2)	−37(2)
W[c,f,h]	OPh	$(CH_2)_4SO$	$9.0(3) \times 10^{-4}$	11.6(4)	−33(1)
W[i]	OMe	Ph_3AsO	2.0(1)	7.1(3)	−33(1)
W[c,i]	OPh	Ph_3AsO	3.1(1)	9.3(3)	−26(1)
W[a]	$SC_6H_2Pr^i{}_3$	$(CH_2)_4SO$	$3.5(1) \times 10^{-2}$	14.6(9)	−16(3)

[a] Ref 13. [b] Ref 5. [c] Ref 9. [d] $k_2^{W}/k_2^{Mo} = 4.6$. [e] $k_2^{W}/k_2^{Mo} = 11$. [f] $k_2^{W}/k_2^{Mo} = 6.0$. [g] $k_2^{OPh}/k_2^{OMe} = 2.4$. [h] $k_2^{OPh}/k_2^{OMe} = 11$. [i] $k_2^{OPh}/k_2^{OMe} = 1.6$. [j] Experimentally determined values.

Rate constants and activation parameters for five reactions (eq 1) and for other oxo transfer reactions previously determined and included for comparison purposes are contained in Table 2. All reactions were found to follow the second-order rate law (eq 3) with rate constants k_2 in the 10^{-2}−10^{-4} M^{-1} s^{-1} range. As for all other oxo transfer reactions mediated by bis(dithiolene)M^{IV} complexes, activation entropies are large and negative, indicative of an associative transition state such as that represented in Figure 1. If this state has the features of that determined from the experimental results for the reduction of $(CH_2)_4SO$ by W^{IV} complexes, it is occurs early in the reaction

(37) Duddeck, H. *Annu. Rep. NMR Spectrosc.* **2004**, *52*, 105−166.

coordinate and is mainly W$\cdots$OSeO_3^{2-} bond-making in character.[12,38]

Complex Structure and Rates. The data of Table 2 reveal that the nature of the axial ligand and the identity of the metal measurably influence reaction rates when other factors are constant. In regard to the indicated axial ligands, the rate order 4 for tungsten complexes and 5 for molybdenum complexes holds for selenate reduction and also applies to the reduction of $(CH_2)_4SO$.[13] Further, $k_2^S/k_2^O = 28$ for the reduction of nitrate to nitrite by **6** and $[W(OC_6H_2\text{-}2,4,6\text{-}Pr^i_3)(S_2C_2Me_2)_2]^{1-}$.[13] The effect is attributed to a more

$$\mathbf{6}\ (SR^*) > \mathbf{4}\ (OPh) > \mathbf{2}\ (OMe) \qquad (4)$$

$$\mathbf{5}\ (SR^*) > \mathbf{3}\ (OPh) \qquad (5)$$

accessible metal site, despite the larger axial ligand substituent R*, which is made possible by the W−S bond length of **6**[11] being 0.46−0.50 Å longer than the W−O bonds of **2** and **4**.[8] The rate constant ratios $k_2^{OPh}/k_2^{OMe} = 1.6$ (Ph_3AsO) and 2.4 (SeO_4^{2-}) for tungsten complexes with the indicated substrates are consistent with the cyclohexane *A* value measure of steric size, which indicates that methoxyl (0.55−0.75 kcal/mol) is comparable with phenoxyl (0.65 kcal/mol).[39] The largest departure of this ratio from unity thus far observed is with $(CH_2)_4SO$ as substrate, for which $k_2^{OPh}/k_2^{OMe} = 11$. Binding through oxygen (or sulfur) is more difficult on a steric basis than for the other two substrates. Last, the ratios $k_2^{W}/k_2^{Mo} = 4.6−11$ are a further demonstration of the *kinetic metal effect* by which tungsten complexes at constant ligation and substrate react faster than molybdenum complexes in substrate reduction by oxo transfer.[9,13,17]

Substrate Reactivity Trends. Sufficient data are now available to allow recognition of certain trends in oxo transfer reactivity of substrate measured by k_2 in acetonitrile with constant metal reactant. Rate order 6 applies wholly or in part to **2**−**6**, with qualification necessary only because not all substrates have been tested with each complex. The less extensive rate order 7 established with tungsten complex **6** affords placement of nitrate before selenate and probably after Ph_3AsO, but this has not been experimentally established. As previous considerations of reaction rates in reductive oxo transfer reveal,[5,9,17] identifying a substrate reactivity trend is much easier than explaining it. The

$$R_3NO > Ph_3AsO > SeO_4^{2-} > (CH_2)_4SO \qquad (6)$$

$$NO_3^{-} > SeO_4^{2-} \approx (CH_2)_4SO \qquad (7)$$

problem lies in the inherent differences in substrate stereochemistry, basicities, and other properties and the fact that the free energies of activation contain substantial enthalpic and entropic contributions which are difficult to evaluate separately. For all but two systems in Table 2, $|T\Delta S^{\ddagger}|$ is 29−58% of $\Delta G^{\ddagger}$. The occurrence of Me_3NO (61 kcal/mol) and $(CH_2)_4SO$ (86 kcal/mol) and the ends of series 6 may be related to the indicated bond dissociation energies, but the position of Ph_3AsO (103 kcal/mol) resists explanation on this basis. The consistent position, $SeO_4^{2-} \gtrsim (CH_2)_4SO$, is difficult to analyze because of the charge difference and the unknown bond-dissociation energy of selenate. We have previously demonstrated the reduction of Ph_2SeO by complex **3** in acetonitrile.[5] Given the usual periodic trend in bond energies, exemplified by $R_3P−S/Se$ bond energy data,[40,41] the order $D(S−O) > D(Se−O)$ is expected. However, we can find no experimental data on Se−O bond energies in organic or inorganic compounds.

Carboxylate Binding. Members of the DMSOR enzyme family assigned under the Hille scheme[2] have been further classified into types I, II, and III on the basis of protein sequence alignments of metal-binding regions.[42] Type II includes, among others, *T. selenatis* SeR, a perchlorate reductase, and membrane-bound respiratory nitrate reductase, which in its entirety contains three subunits and is designated NarGHI. The defining feature of type II is a highly conserved Asp residue which is postulated to function as a ligand at the molybdenum site. Binding of the Asp carboxylate group in two molybdenum site structures in the catalytic subunit NarG has been confirmed by crystallography. The structure of *E. coli* NarGH[42] contains the oxidized site $\{Mo^{VI}O(O_2C{\cdot}Asp)(S_2pd)\}$ with bond distances of Mo−S = 2.45 Å (mean) and Mo═O = 1.8 Å and η^1-*syn*-carboxylate coordination. The structure of *E. coli* NarGHI,[43] determined before the NarGH result, is reported to contain a $\{Mo(O_2C{\cdot}Asp)(S_2pd)_2\}$ site with distorted trigonal prismatic geometry, Mo−S ≈ 2.4 Å, and unsymmetrical η^2-carboxylate binding reflected by Mo−O ≈ 1.9 and 2.4 Å. The unit is presumed to contain Mo^{VI}, but the apparent absence of an oxo ligand renders this oxidation state suspect: Mo^{IV} or Mo^{V} is more appropriate. Both types of carboxylate binding are precedented;[44,45] however, nitrate reductase is the first example of carboxylate coordination to molybdenum in proteins. Although the sequence alignment comparison raises the possibility of an Asp ligand in SeR, none was found in the structure of *T. selenatis* SeR, deduced from XAS.[20] Further, the enzyme is specific for selenate; nitrate reductase activity was not detected,[15] and nitrate reductases are described as ineffective in selenate reduction.[16]

Sequence alignment considerations do not appear to apply in the case of *T. selenatis* SeR, but this is the only SeR on

(38) Note that DFT calculations on the systems $[M^{IV}(OMe)(S_2C_2H_2)_2]^{1-}/Me_2SO$ (M = Mo, W) predict a later transition state with appreciable M$\cdots$O bond making and S$\cdots$O bond weakening and a geometry approaching that of $W^{VI}O$ complex **9** or **10**.[28]

(39) Anslyn, E. V.; Dougherty, D. A. *Modern Physical Organic Chemistry*; University Science Books: Sausalito, CA, 2004; p 104.
(40) Holm, R. H.; Donahue, J. P. *Polyhedron* **1993**, *12*, 571−589.
(41) Capps, K. B.; Wixmerten, B.; Bauer, A.; Hoff, C. D. *Inorg. Chem.* **1998**, *37*, 2861−2864.
(42) Jormakka, M.; Richardson, D.; Byrne, B.; Iwata, S. *Structure* **2004**, *12*, 95−104.
(43) Bertero, M. G.; Rothery, R. A.; Palak, M.; Hou, C.; Lim, D.; Blasco, F.; Weiner, J. H.; Strynadka, N. C. J. *Nature Struct. Biol.* **2003**, *10*, 681−687.
(44) Carrell, C. J.; Carrell, H. L.; Erlebacher, J.; Glusker, J. P. *J. Am. Chem. Soc.* **1988**, *110*, 8651−8656.
(45) Holm, R. H.; Kennepohl, P.; Solomon, E. I. *Chem. Rev.* **1996**, *96*, 2239−2314.

Table 3. Bond Distances (Å) and Angles (deg) of $[Mo(O_2CR)(S_2C_2Me_2)_2]^{1-}$ Complexes

	R = Ph	R = Bu$^{t\,f}$
Mo−O1	2.189(2)	2.19(1)
Mo−O2	2.205(2)	2.17(1)
Mo−S^a	2.332(6)	2.32(2)
S−C^a	1.755(4)	1.78(2)
C−C^b	1.34(1)	1.32(2)
S1−Mo−S2	81.19(3)	82.4(2)
S3−Mo−S4	81.60(3)	81.4(2)
S1−Mo−S4	84.41(3)	83.0(1)
S2−Mo−S3	84.74(3)	85.4(2)
S1−Mo−S3	137.20(3)	138.2(2)
S2−Mo−S4	140.92(3)	140.4(2)
O1−Mo−O2	60.64(9)	60.2(4)
O1−C9−O2	119.4(3)	119(2)
O1−Mo−S1	132.51(7)	130.1(3)
O1−Mo−S2	88.32(7)	86.6(3)
O1−Mo−S3	86.89(7)	88.6(3)
O1−Mo−S4	127.01(7)	129.9(3)
O2−Mo−S1	90.87(6)	89.3(3)
O2−Mo−S2	128.48(7)	127.1(3)
O2−Mo−S3	128.49(6)	128.9(3)
O2−Mo−S4	87.68(6)	89.2(3)
MoS1S2/MoO1O2^c	119.3(1)	116.8(3)
MoS3S4/MoO1O2^c	115.6(1)	117.9(3)
δ^d	0.816(1)	0.807(3)
θ^e	125.0(1)	125.2(2)

^{a} Mean of four. ^{b} Mean of two. ^{c} Dihedral angle. ^{d} Displacement Mo atom from MoS_4 mean plane. ^{e} Dihedral angle of MoS_2 planes. ^{f} Data for one of four independent anions, all of which are dimensionally very similar.

which there is any active site structural information. To establish possible structural analogues of the reduced sites of selenate, nitrate, and perchlorate reductases with carboxylate ligands and to investigate any accompanying reactivity in substrate reduction, we have prepared the Mo^{IV} carboxylate complexes **7** and **8** in ca. 70% yield by the procedure in Figure 2. The two complexes are isostructural; metric features of both are collected in Table 3, and the structure of **8** is provided in Figure 5. The complexes are six-coordinate with trans ligand angles of 137.0−141.9°, indicating a close approach to idealized trigonal prismatic geometry. The molybdenum atoms are displaced 0.81−0.82 Å toward the carboxylates, which bind as symmetrical η^2-ligands with Mo−O distances of 2.17−2.21 Å. Chelate rings are canted at a dihedral angle of 125°; mean Mo−S distances are 2.32−2.33 Å. These complexes are isostructural with the corresponding species $[W(O_2CR)(S_2C_2Me_2)_2]^{1-}$.[10,11] The structures of **7** and **8** are taken to represent unconstrained versions of the (apparently reduced) site of NarGHI. Further, complex **13**, for which W−S = 2.41−2.45 Å, W=O = 1.72 Å, W−O = 2.07 Å, and trans S−W−S = 143.5°,[11] should fulfill the same role for the oxidized NarG site.

To investigate the effect of carboxylate and other axial ligands on reactivity, additional systems were investigated using W^{IV} complexes (1−6 mM), because of the greater ease of oxidation and stability of possible $W^{VI}O$ products, and selenate and perchlorate (3−20 equiv) as potential substrates in acetonitrile. Systems were monitored by UV−vis spectrophotometry and ^{1}H NMR for periods up to 20 h at room temperature. Under these conditions, oxo transfer reactions of complexes such as **1**−**6** with *N*-oxides, *S*-oxides, nitrate, and selenate readily proceed. Perchlorate was included to search for perchlorate reductase activity.[46,47] Observations are briefly summarized as follows: **4**/ClO_4^-, no appreciable reaction; **8**/ClO_4^-, reaction but **13** could not be identified; **14**/SeO_4^{2-}, unidentified reaction, trace of $W^{VI}O$ product (in aqueous solution with Na_2SeO_4 a green-blue precipitate formed); **14**/ClO_4^-, nil reaction. The W^{IV} complex **14**[23] was examined because it represents an unprotonated version of the active site of reduced SeR (Figure 1), which could be reactive in selenate reduction. Carboxylate complexes can sustain oxo transfer reactions, as shown by the synthesis of (Et_4N)[**13**] (41%) from **8** and Ph_3AsO.[11] However, when the system **8**/Ph_3AsO was examined at the dilute concentrations appropriate for kinetics determination, spectral complexity indicated more than one reaction.

Summary. The following are the principal results and conclusions of this investigation.

(1) The square pyramidal complexes $[M^{IV}(OMe)(S_2C_2Me_2)_2]^{1-}$ (M = Mo, W) have been prepared as analogues of the reduced site in *T. selenatis* selenate reductase, which, from Mo EXAFS analysis, contains two pyranopterindithiolene ligands and an axial hydroxide. The Mo−OMe distance of 1.862 Å provides a measure of the expected Mo−OH bond length in the enzyme, whose reported value may be artifactually long.

(2) Bis(dithiolene) complexes, $[M^{IV}L(S_2C_2Me_2)_2]^{1-}$ (M = Mo, W; L = RO^-, R^*S^-, cleanly reduce selenate to selenate in second-order oxygen atom transfer reactions that proceed through associative transitions states such as that illustrated in Figure 1. We are unaware of any previous nonenzymatic reactions resulting in reduction of selenate by oxo transfer.

(3) Second-order rate constants for the reactions (1) cover the range of 3.6×10^{-2} to 7.2×10^{-4} M^{-1} s^{-1}, are dependent upon axial ligand (series 4 and 5), and manifest the kinetic metal effect in substrate reduction ($k_2^{W} > k_2^{Mo}$). Comparison with previous results leads to recognition of substrate reactivity trends (series 6 and 7) which, however, are not easily explained in their entirety.

(4) The $[Mo^{IV}(O_2CR)(S_2C_2Me_2)_2]^{1-}$ complexes are readily prepared, have approximate trigonal prismatic stereochemistry with symmetrical η^2-carboxylate binding, and are unconstrained structural analogues of the reduced site in the Nar nitrate reductase and, perhaps, also of sites in selenate and perchlorate reductases if sequence alignment arguments apply.

(5) The complexes in (2) are capable of reducing at least four types of biological substrates (*N*-oxides, *S*-oxides, nitrate, selenate) in oxo transfer reactions, all of which have the characteristics in (2). Analoguous reaction systems cannot

(46) Kengen, S. W. M.; Rikken, G. B.; Hagen, W. R.; van Ginkel, C. G.; Stams, A. J. M. *J. Bacteriol.* **1999**, *181*, 6706−6711.
(47) Okeke, B. C.; Frankenberger, W. T., Jr. *Microbiol. Res.* **2003**, *158*, 337−344.

prove an enzyme pathway or mechanism but can disclose what is possible. Given the close structural relationship of analogue complexes and the immediate coordination environment of enzyme sites in the same oxidation state, enzymatic transformation of the substrates by atom transfer is highly probable. With one DMSOR, this reaction has been proven by isotope labeling.[48]

(48) Schultz, B. E.; Holm, R. H.; Hille, R. *J. Am. Chem. Soc.* **1995**, *117*, 827−828.

Acknowledgment. This research was supported by NSF Grant CHE 0237419. C.T. was supported by a fellowship from the Quebec Nature and Technology Research Fund.

Supporting Information Available: X-ray crystallographic files in CIF format for the structure determinations of the compounds in Table 1. This material is available free of charge via the Internet at http://pubs.acs.org.

IC0521630